

Supporting information

Nano-visualization of Hydrogel Dynamics via Surface Plasmon-Enhanced Aggregation-Induced Emission

Qing-Bo Liang, †^a Zhao Li, †^a Yu-Hua Weng, ^a Lang Chang, ^a Jia-Dai Wang, ^a Ting-Bin Wen, ^a Shuo-Hui Cao, ^{*abc} and Yao-Qun Li ^{*a}

- a. Department of Chemistry and the MOE Key Laboratory of Spectrochemical Analysis & Instrumentation, College of Chemistry and Chemical Engineering, Xiamen University, Xiamen 361005, P. R. China.
- b. Department of Electronic Science, Xiamen University, Xiamen 361005, P. R. China.
- c. Shenzhen Research Institute of Xiamen University.

Table of content

1. Materials and Methods
2. Supporting Figures
3. References

1. Materials and Methods

1.1 Reagents and materials

Poly(vinyl alcohol) (PVA, MW: 13000-23000, Sinopharm Chemical Reagent Co, Ltd). Poly (acrylic acid) (PAA, MW: ~450000, Adamas). Rhodamine B isothiocyanate (RBITC, Sigma-Aldrich). 5-(4-(diphenylamino)phenyl)thiophene-2-carbaldehyde (Zancheng (Tianjin) Technology Co., Ltd). 1,4-dimethylpyridin-1-ium iodide (Bide Pharmatech Co., Ltd). KPF₆ (Shanghai Aladdin Biochemical Technology Co., Ltd). Piperidine, acetone, dichloromethane, ethanol, dimethyl sulfoxide, 1,4-dioxane, and acetonitrile were analytically pure (Sinopharm Chemical Reagent Co., Ltd). Rhodamine B (RhB, Sinopharm Chemical Reagent Co, Ltd). Coverslip (FIS12-545-102; Fisherbrand). Ultrapure water was obtained from Milli-Q, Xiamen University.

1.2 Instruments

A laboratory-built multifunctional fluorescence spectrometer was employed to acquire the fluorescence spectra of TTPy in solution. [1] Characterization of the hydrogel chips—including the collection of fluorescence microscopy images, SPCE incidence angle scanning curves, and emission spectra—was conducted on a custom angle scanning-surface plasmon coupled emission (AS-SPCE) microscopy platform, detailed in Figure S1.[2-3] The microscope was equipped with an oil-immersion objective (100×, NA 1.49, Nikon). A half-wave ($\lambda/2$) plate was rotated to alternate the excitation polarization alternatingly between s- and p-states. The incident angle was precisely scanned from 0° to 80° (where 0° represents the epifluorescence configuration) by adjusting the mirror position within the illuminator.

1.3 Reflectivity simulation

Optical simulations were performed using WinSpall software with a four-layer Fresnel model parameterized by thickness, refractive index, and light polarization. [2] Due to the non-covalent and mobile nature of TTPy, combined with the network relaxation and homogenization of the hydrogel during swelling, a near-uniform vertical distribution of refractive index is expected for the hydrogel layer. Therefore, a uniform refractive index profile was assumed in the simulations.

1.4 Synthesis of TTPy

As shown in Figure S2, TTPy was synthesized following the established method. A mixture of 5-(4-(diphenylamino)phenyl)thiophene-2-carbaldehyde (71 mg, 0.2 mmol) and 1,4-dimethylpyridin-1-ium iodide (56.4 mg, 0.24 mmol) was placed in a two-necked flask. Anhydrous ethanol (9 mL) and piperidine (2 drops) were added, and the reaction was refluxed overnight under nitrogen protection. After cooling to room temperature, partial solvent removal was achieved via rotary evaporation. Anhydrous diethyl ether was then added to the residue, inducing the formation of a deep red precipitate, which was collected by filtration. The precipitate was redissolved in acetone and mixed with a saturated KPF₆ solution (3 mL). After stirring for 1 h, acetone was removed by rotary evaporation. The resulting red precipitate was filtered, washed with water, and dried under vacuum to yield the crude product. The crude product was purified via neutral alumina column chromatography, using a dichloromethane-methanol mixture (85:15 v/v) as the eluent. The solvent was removed under reduced pressure to give a red powder TTPy. ¹H NMR (400 MHz, DMSO): δ 8.79 (d, J = 5.2 Hz, 2H), 8.20 (s, 1H), 8.18 - 8.13 (m, 2H), 7.63 (d, J = 6.7 Hz, 2H), 7.53 - 7.47 (m, 2H), 7.36 (t, J = 6.2 Hz, 3H), 7.13 (d, J = 6.4 Hz, 2H), 7.12 - 7.06 (m, 4H), 6.99 (d, J = 6.9 Hz, 2H), 4.21 (s, 3H). As shown in Figure S2c, the hydrodynamic size distribution of TTPy aggregates exhibits a peak at 156.9±8.6 nm

1.5 Preparation of the metal substrate

The metal substrate was prepared by magnetron sputtering. Before magnetron sputtering, the round coverslips (25 mm diameter) were soaked in a chromic acid wash solution for 12 h. Then, the coverslips were cleaned by ultrasonic cleaning with ultrapure water, ethanol, and acetone in turn. Finally, the coverslips were blown dry with nitrogen. The pre-cleaned round coverslips were deposited with 2 nm Cr and 30 nm Au by magnetron sputtering to prepare the

metal substrate. The 2 nm Cr layer can promote the adhesion of the Au film to the coverslip. The magnetron sputtering of the metal substrate was prepared by the magnetron sputtering coating system (Exploror-14) of the Pen-Tung Sah Institute of Micro-Nano Science and Technology, Xiamen University.

1.6 Preparation of AIE hydrogel-modified SPCE substrate

PVA was dissolved in ultrapure water by heating and stirring at 85-90 °C. PAA was dissolved in ultrapure water by stirring. The two solutions were then homogeneously mixed, followed by the addition of a DMSO solution containing TTPy. The mixture was reacted at 60 °C for 5 h to obtain a 3 wt% PAA/3 wt% PVA pre-gel solution containing 60 μM TTPy. The TTPy/PAA/PVA pre-gel solution was diluted with a DMSO/H₂O mixture and spin-coated onto an Au substrate. To cross-link the gel, the chip was thermally treated at 150 °C for 40 minutes.

1.7 Preparation of AIE hydrogel-modified glass substrate

PVA was dissolved in ultrapure water by heating and stirring at 85-90 °C. PAA was dissolved in ultrapure water by stirring. The two solutions were then homogeneously mixed, followed by the addition of a DMSO solution containing TTPy. The mixture was reacted at 60 °C for 5 h to obtain a 3 wt% PAA/3 wt% PVA pre-gel solution. The glass substrate was pre-treated by soaking in piranha solution for 40 minutes, then washed with ultrapure water and dried. The PAA/PVA pre-gel solution was diluted with a DMSO/H₂O mixture and spin-coated onto the cleaned glass substrate. To cross-link the gel, the chip was thermally treated at 150 °C for 40 minutes.

1.8 Preparation of RhB hydrogel-modified glass substrate

PVA was dissolved in ultrapure water by heating and stirring at 85-90 °C. PAA was dissolved in ultrapure water by stirring. The two solutions were then homogeneously mixed, followed by the addition of a water solution containing RhB. The mixture was reacted at 60 °C for 5 h to obtain a 3 wt% PAA/3 wt% PVA pre-gel solution containing 60 μM RhB. The RhB/PAA/PVA pre-gel solution was diluted with a DMSO/H₂O mixture and spin-coated onto an Au substrate. To cross-link the gel, the chip was thermally treated at 150 °C for 40 minutes.

1.9 AIE properties measurement

DMSO/H₂O mixtures with different water fractions (WF) were used to evaluate the AIE properties of TTPy. With increasing WF, a progressive enhancement of emission intensity accompanied by a spectral blue shift was observed (Figure S3b), which is attributed to the restricted molecular rotation during aggregate formation. The emission properties of TTPy were further investigated in solvents of different polarities, with the strongest fluorescence emission of TTPy observed when DMSO was used as a good solvent (Figure S3c).

Supporting Figures

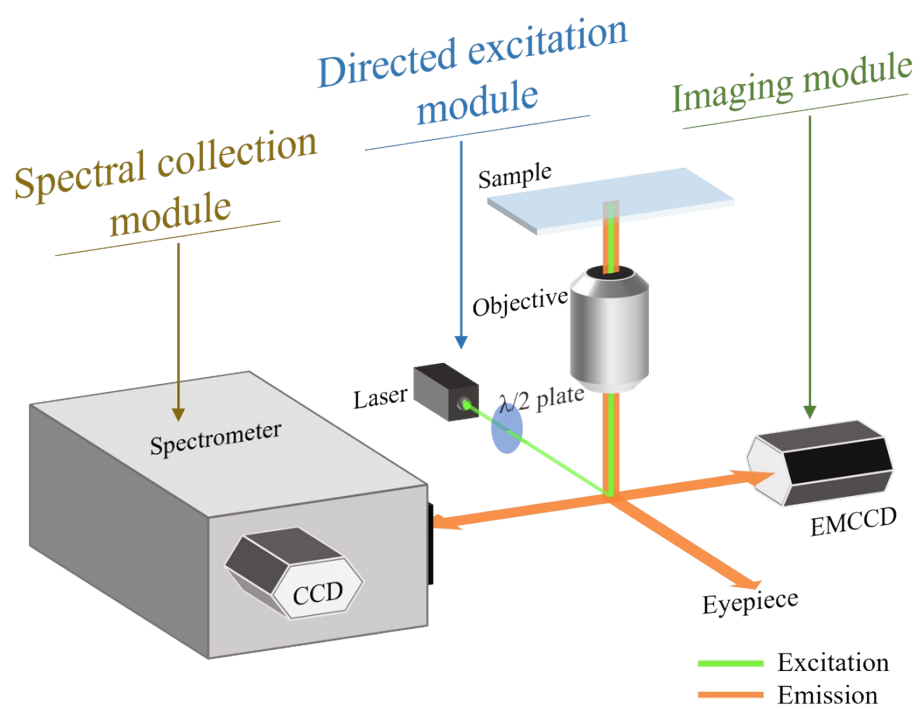


Figure S1. Schematic diagram of the AS-SPCE microscopy system.

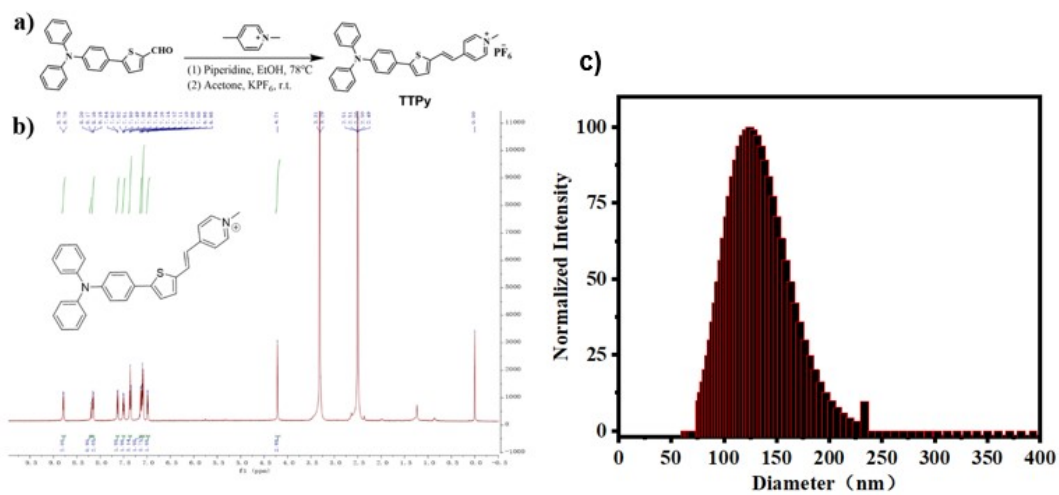


Figure S2. (a) Synthesis route of TTPy. (b) ¹H NMR spectrum of TTPy. The inset shows the structural formula of the TTPy molecule. (c) Size distribution of TTPy aggregates measured by dynamic light scattering.

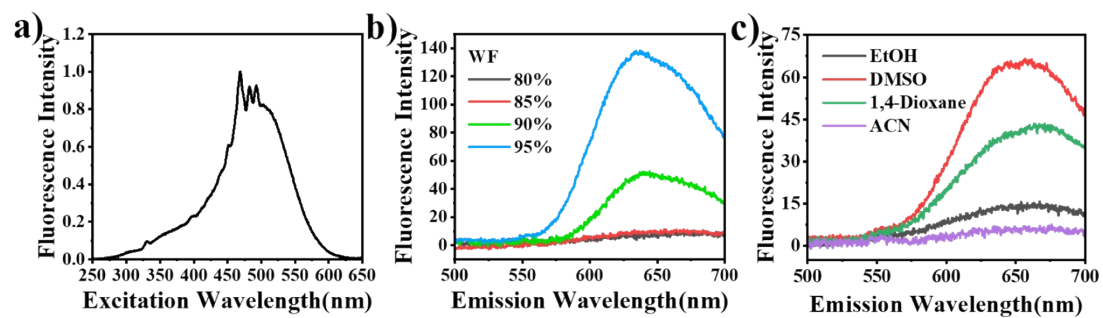


Figure S3. (a) Excitation spectrum ($\lambda_{em}=667$ nm) of TTPy ($10 \mu\text{M}$) in DMSO/ H_2O mixture with water fraction (WF)=90%. (b) Emission spectra ($\lambda_{ex}=467$ nm) of TTPy ($10 \mu\text{M}$) in DMSO/ H_2O mixture with different WFs. (c) Emission spectra ($\lambda_{ex}=467$ nm) of TTPy ($10 \mu\text{M}$) in different solvent/water mixtures with WF=95%.

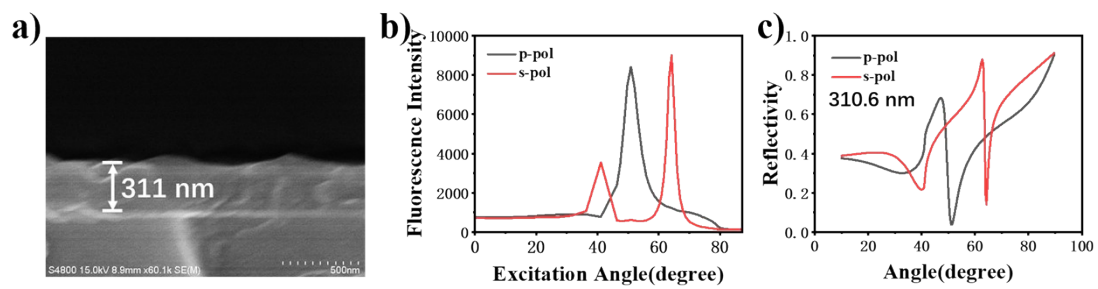


Figure S4. Characterization of the dry AIE hydrogel film. (a) Cross sectional SEM image. (b) Experimental SPCE excitation angular distributions. (c) Corresponding theoretical reflectivity curves.

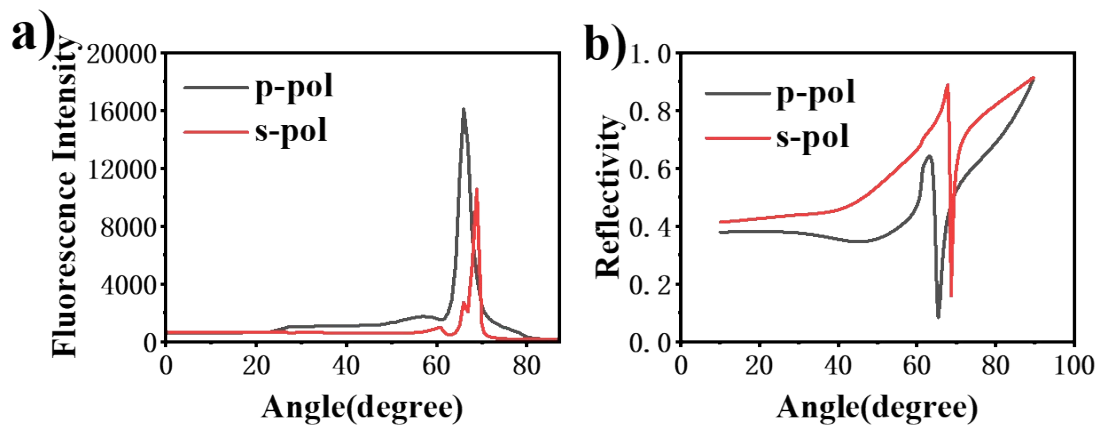


Figure S5. Experimental and simulated SPCE angle profiles of the AIE hydrogel in pH 6.0 solution. (a) Measured SPCE excitation angle distributions. (b) Theoretical reflectivity curves to simulate the SPCE profiles obtained using Winspall software. The experimental data show a well-defined directional profile and are in close agreement with the simulation.

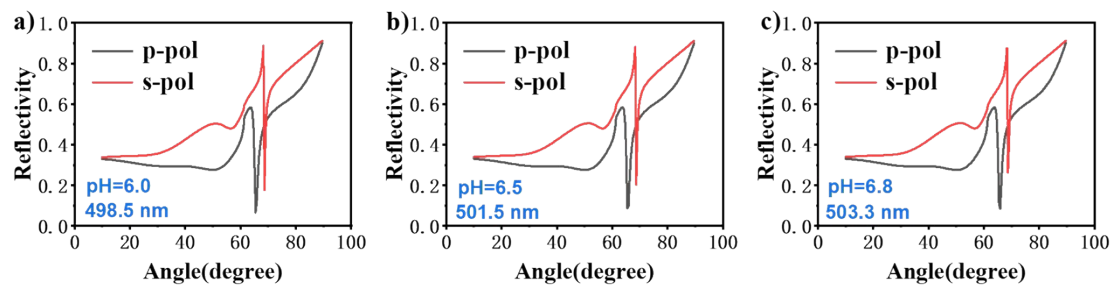


Figure S6. Simulated reflectivity curves for the hydrogel at varying pH values. The curves correspond to the angular distributions at (a) pH 6.0, (b) 6.5, and (c) 6.8.

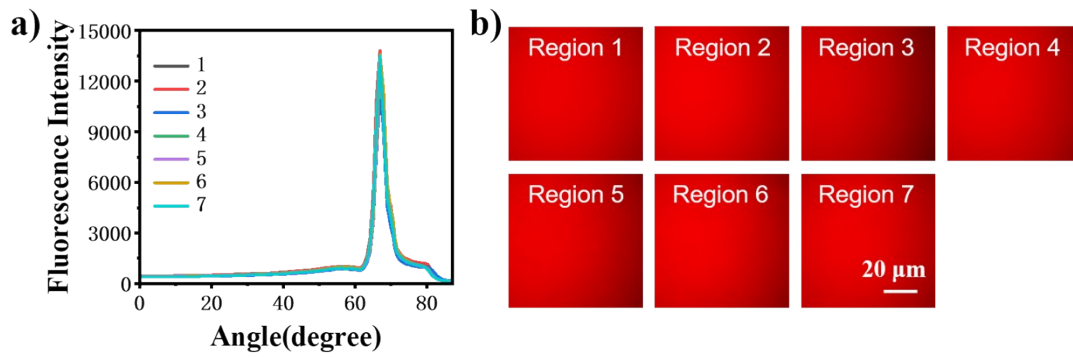


Figure S7. AIE hydrogel microdomains measurements (All in PBS, pH 7.04). (a) S-polarized excitation angular distribution across different microdomains. (b) Fluorescence microscopy images of distinct microdomains at 66° incidence angle.

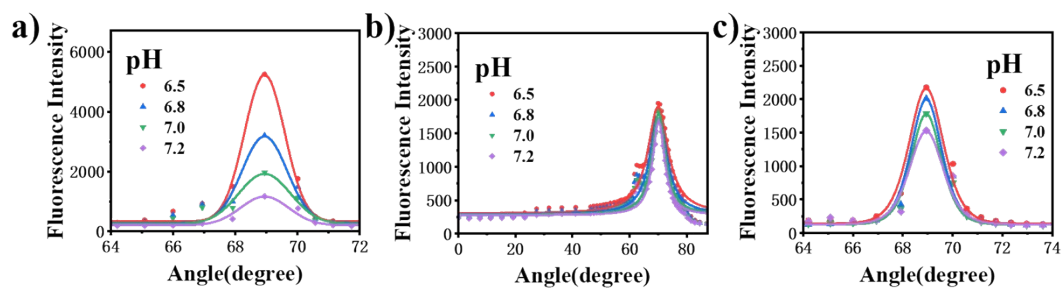


Figure S8. Comparative analysis of excitation angular distributions across different platforms. S-polarized excitation angular distributions were measured in solutions of varying pH for three systems: (a) AIEgen-doped hydrogel on a gold substrate, (b) AIEgen-doped hydrogel on a non-plasmonic glass substrate, and (c) RhB-doped hydrogel on a gold substrate.

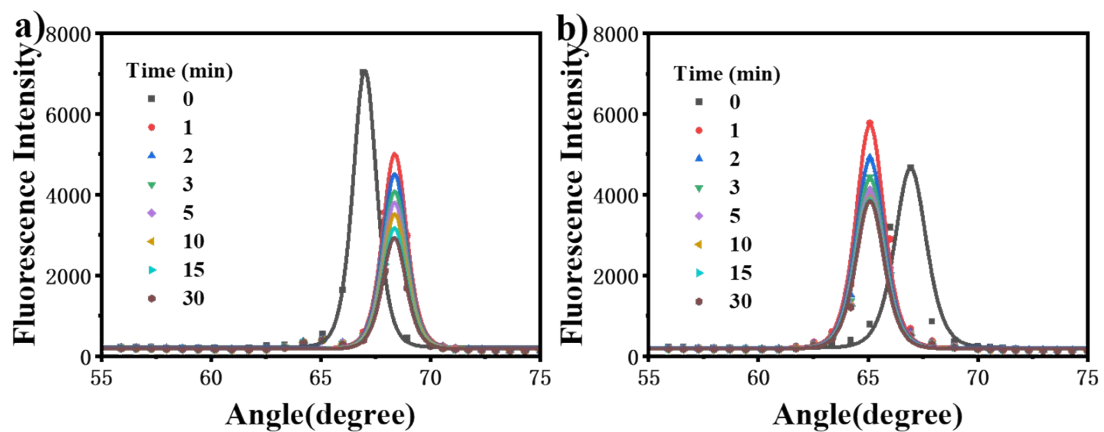


Figure S9. Real-time monitoring of the excitation angular distributions of a hydrogel during alternating pH exposure. The response was tracked (a) during the transition from pH 1.0 to 7.0 and (b) during the reverse transition from pH 7.0 to 1.0.

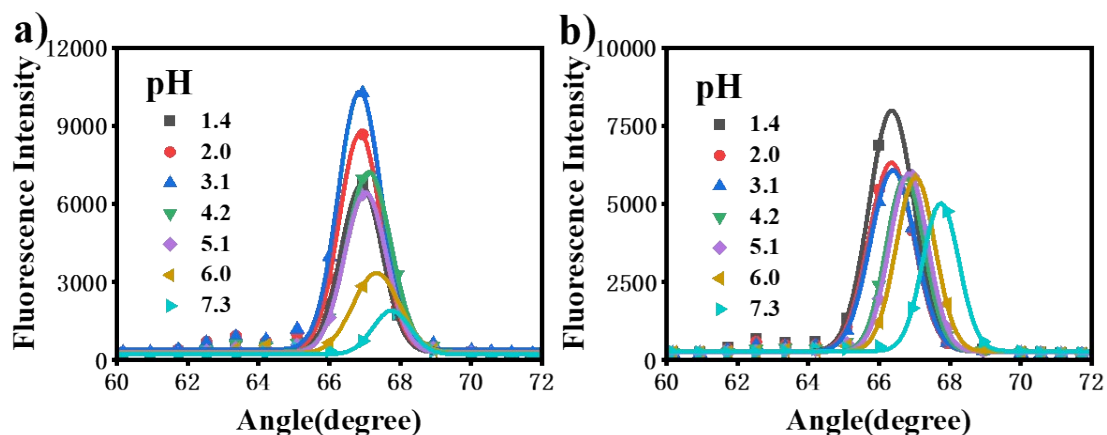


Figure S10. Excitation angular distributions of the hydrogel under different pH conditions and pH gradients: (a) acidic to neutral and (b) neutral to acidic.

3. References

- [1] J.-W. Wei, J.-R. He, S.-Y. Chen, Y.-H. Guo, X.-Z. Huo, N. Zheng, S.-H. Cao, Y.-Q. Li, Synchronous fluorescence spectra-based machine learning algorithm with quick and easy accessibility for simultaneous quantification of polycyclic aromatic hydrocarbons in edible oils, *Food Control* 2024, **158**, 110205.
- [2] M. Chen, X.-H. Pan, Q. Liu, S.-X. Huo, S.-H. Cao, Y.-Y. Zhai, Y. Zhao, Y.-Q. Li, Variable-angle nanoplasmonic fluorescence microscopy: An axially resolved method for tracking the endocytic pathway, *Anal. Chem.* 2019, **91**, 13658-13664.
- [3] X. H. Pan, M. Chen, S. H. Cao, Z. Q. Xu, Z. Li, Y. Q. Li, Plasmon Coupling Enhanced Micro-Spectroscopy and Imaging for Sensitive Discrimination of Membrane Domains of a Single Cell, *Chem. Eur. J.* 2021, **27**, 17331-17335.